

## Tail Event Driven Networks of SIFIs

Cathy Yi-Hsuan Chen, Wolfgang Karl Härdle, Yarema Okhrin

### Angaben zur Veröffentlichung / Publication details:

Chen, Cathy Yi-Hsuan, Wolfgang Karl Härdle, and Yarema Okhrin. 2017. "Tail Event Driven Networks of SIFIs." *SSRN Electronic Journal*, 1–33. <https://doi.org/10.2139/ssrn.3085850>.

### Nutzungsbedingungen / Terms of use:

licgercopyright

Dieses Dokument wird unter folgenden Bedingungen zur Verfügung gestellt: / This document is made available under these conditions:

**Deutsches Urheberrecht**

Weitere Informationen finden Sie unter: / For more information see:

<https://www.uni-augsburg.de/de/organisation/bibliothek/publizieren-zitieren-archivieren/publiz/>



# Tail event driven networks of SIFIs

Cathy Yi-Hsuan Chen\*  
Wolfgang Karl Härdle\*  
Yarema Okhrin\*<sup>2</sup>



\*Humboldt-Universität zu Berlin, Germany

\*<sup>2</sup> University of Augsburg, Germany

This research was supported by the Deutsche  
Forschungsgemeinschaft through the SFB 649 "Economic Risk".

<http://sfb649.wiwi.hu-berlin.de>  
ISSN 1860-5664

SFB 649, Humboldt-Universität zu Berlin  
Spandauer Straße 1, D-10178 Berlin



# Tail event driven networks of SIFIs

Cathy Yi-Hsuan Chen\*, Wolfgang Karl Härdle†, Yarema Okhrin‡

## Abstract

The interdependence, dynamics and riskiness of financial institutions are the key features frequently tackled in financial econometrics. We propose a Tail Event driven Network Quantile Regression (TENQR) model which addresses these three aspects. More precisely, our framework captures the risk propagation and dynamics in terms of a quantile (or expectile) autoregression involving network effects quantified through an adjacency matrix. To reflect the nature and risk content of systemic risk, the construction of the adjacency matrix is suggested to include tail event covariates. The model is evaluated using the SIFIs (systemically important financial institutions) identified by the Financial Stability Board (FSB) as main players in the global financial system. The risk decomposition analysis of it identifies the systemic importance of SIFIs and thus provides measures for the required level of additional loss absorbency. It is discovered that the network effect, as a function of the tail probability, becomes more profound in stress situations and brings the various impacts to the SIFIs located in different geographic regions.

*JEL classification:* C01, C14, C58, C45, G01, G15, G31

*Keywords:* systemic risk; network analysis; network autoregression; tail event

---

\*Humboldt-Universität zu Berlin, C.A.S.E. - Center for Applied Statistics and Economics, Spandauer Str. 1, 10178 Berlin, Germany and Department of Finance, Chung Hua University, No. 707, Sec. 2, WuFu Rd., Hsinchu, Taiwan 30012

†Humboldt-Universität zu Berlin, C.A.S.E. - Center for Applied Statistics and Economics, Spandauer Str. 1, 10178 Berlin, Germany and School of Business, Singapore Management University, 50 Stamford Road, Singapore 178899

‡Chair of Statistics, Faculty of Business and Economics, University of Augsburg, 86159 Augsburg, Germany

# 1 Introduction

Systemic risk threatens financial stability and the functioning of financial markets due to shocks on liquidity, reduced market confidence and willingness of risk taking. A growing body of literature discusses macroprudential risk management approaches to study systemic risk with two goals: ensuring financial stability and quantify a risk charge proportional to the relative systemic contribution. Both goals are targeted to inject additional capital into the financial system to make it more resilient. However, as pointed out by Bluhm and Krahnen (2014) macroprudential monitoring is still at a very early stage, quantifying the magnitude of systemic risk and identifying systemically relevant contributors need more scientific analysis. Without such effort, the supervisory authorities face difficulties either to set proper capital requirements as a risk buffer against adverse shocks for every financial institutions or to calculate additional risk charges for systemically important financial institutions (SIFIs) for their extra negative externalities on the financial system.

In order to understand the interconnectedness among SIFIs from a system-wide perspective, one has to study the measure, the degree, and asymmetric nature of systemic risk. To do so we propose a quantitative and system-wide framework based on a topological network methodology. Network analysis is quite capable of portraying the interplay among financial institutions and measuring their interconnectedness (see Diebold and Yilmaz, 2014; Barigozzi and Brownlees, 2016). Summarizing their arguments, interconnectedness of financial institutions on the interbank market is an absolute key to understanding systemic risk. Interconnectedness captures the situations when financial distress in one institution subsequently raises the likelihood of financial distress in other institutions because of their network of contractual relations and interbank lending among them, leading to a “too-interconnected-to-fail” situation. The complexity of the connections brings challenges to researchers, fortunately the network analysis ideally presents the interconnections of a large panel as a graph where the nodes represent the variables/output in the panel, and the edges between each pair of nodes denote their dependencies corresponding to the variables.

This study proposes modern network techniques for the analysis of dynamic interconnect-

edness of SIFIs in five aspects. First, we concentrate on the network of SIFIs due to their systemic relevance. The interconnectedness of SIFIs' network shall be quantified and kept monitored. Second, we propose and argue that a network (or “adjacency matrix”) should be based on tail event measures. The adjacency matrix is constructed by the similarity of risk profiles of node pairs. The risk profile comprising of various tail risk variables is more capable to portray the risk structure and represent the diverse risk contents.

Third, the identified SIFIs by Financial Stability Board (FSB) will be allocated to different buckets depending on their scores of policy measures proposed by Basel Committee on Banking Supervision (BCBS) to admit that each SIFI potentially creates different degrees of contagion. The five buckets correspond to the additional loss absorption capacities from 1% to 3.5% to ensure the sufficiency of their common equities in case of the default. However, the methodology proposed by BCBS depends very much on the choice of policy measures and threshold of scores. Therefore, we present a parsimonious and intuitive metric for the “aggregate risk” in a network comprised of related entities to quantify the systemic risk, the resulting systemic risk scores can be used to monitor systemic vulnerability. The risk decomposition from the aggregate systemic risk quantifies the risk contribution of each node. This way one may study the sensitivity by injecting nodal risk. For a supervisory purpose, a node with a high degree of connectedness may thus be monitored more carefully for higher risk increments. In a nutshell, this analytic decomposition enables identifying the source of systemic vulnerabilities.

Fourth, the responses/outputs at the network vertices constitute an ultrahigh dimensional vector, that is, the returns of the defined SIFIs. The interest of our analysis lies in the extremes or higher moments, see Härdle et al. (2016), Fan et al. (2016). Given an adjacency matrix one is interested in how a stress loaded in one node (or a collection of these) propagates through a network. The basic idea is seeded in the CoVaR concept of Adrian and Brunnermeier but needs an extension to a dynamic framework also portraying node-specific features. In order to study tail event risk transmission in a dynamic context we propose “Tail Event driven Network Quantile Regression” (TENQR) model, extending the variation about the mean analysis of Zhu et al. (2017). The technique presented here is similar to Zhu et al. (2016), but different in the construction of the adjacency matrix as we will see later. In a TENQR framework, after controlling node-specific

feature, autoregressive impact and the market-wide covariates, the response of SIFIs given a range of quantile levels or  $\tau$  values can be governed by the network factor as an indicator of the degree of connectedness in the system. The coefficient curve at multiple percentiles exhibits a downward slope (in European and in the US) to signal an asymmetric reaction strongly toward to lower quantiles, or a U-shape (in Asia) to indicate an equivalent importance between lower and upper tail. An investigation by means of moving window estimation depicts the surface comprised of time-varying coefficient curves derived from quantile regression, indicating that the network factor contributes to residual return predictability more profoundly in economic downturn and less in the rest of periods. The TENQR model does align with the nature of systemic risk that has (i) large impact, particular in the downside constituting an asymmetric reaction; (ii) widespread coverage that can be examined through a panel or stack model; (iii) a ripple effect being detected by an intertemporal investigation.

Fifth, we show the geographic vulnerability with respect to systemic risk. It's worthwhile to discuss the geographic distinctions since each region has distinct economic characteristics, including the structure of its financial system, its position in the global village, and the nature of its ongoing financial consolidation. These characteristics may define the geographic frailty of financial risk. For this reason we consider the pooled quantile regressions for the SIFIs from the US, Europe and Asia. In doing so, one may know which region is more sensitive to the network factor. With this understanding, the impact caused by a systemic network is likely to be region-specific. Some regions play as risk transmitters, while others play as risk recipients. For a supervisory purpose, the region characterized as a main risk transmitter should be closely monitored, while others receiving risk are suggested to preserve more capital as systemic risk buffer. Besides, the implied vulnerabilities across regions are in accordance with the results of systemic risk decomposition.

Having these efforts, we contribute to a “manageable” systemic risk: the supervisors are able to rank the systemic importance for each SIFIs, to measure the resulting connectedness in a system, and to evaluate the impact of network on the conditional quantile of a response. In the next section we discuss the construction of the adjacency matrix and its relevance for the systemic risk score. Section 3 contains the details for the network

quantile regression. Section 4 concludes.

## 2 Adjacency matrix and systemic risk score

### 2.1 Financial characteristics of SIFIs

As institutions grow in size, interconnectedness and complexity, they profit by lower funding cost and economy of scale. However, the moral-hazard problems or so called “negative externalities” subsequently raise because governments have been forced to use public funds to support distressed financial institutions, leading to a “too-interconnected-to-fail” or “too-big-to-fail” situation. Due to the importance of SIFIs for market stability measuring systemic risk for its interconnectedness and detecting the major contributors are urgent issues. Hence, we concentrate on 28 global SIFIs (or called G-SIB) listed and updated in Nov. 2015 by FSB, but disregard two SIFIs, Agriculture Bank of China and Banque Populaire CE, due to their relative shorter data periods. Daily data such as daily stock return and implied volatility have been collected ranging from Jan. 2007 to Dec. 2015.

In Table 1, we list the names of the SIFIs with the corresponding index numbers assigned in this research, and summarize the bank-specific attributes such as debt ratio, firm size, country where the headquarter is located and the buckets assigned by BCBS. Debt ratio, a ratio of total debt to total asset, captures the fragility of a bank, while the size, as total assets, proxies for the bank being too big to fail. In particular, size risk is the most determinant standalone bank risk in relation to systemic risk (Laeven et al., 2015).

These balance sheet data are available usually yearly. Each just released piece of balance sheet information enters the TENQR model to obtain results in real time. The bucket approach is defined in Table 2 of the Basel Committee document *Global systemically important banks: updated assessment methodology and the higher loss absorbency requirement*, July 2013, which is designed to reduce the moral-hazard problems and systemic risk by requiring additional common equity loss absorbency as a percentage of risk-weighted assets that applies to each SIFI from 3.5% (Bucket 5), 2.5% (Bucket 4), 2.0% (Bucket 3),

1.5% (Bucket 2) to 1% (Bucket 1). Later, the effectiveness of the bucket method can be justified through the risk decomposition analysis.

## 2.2 Similarity matrix

Graph theory is very useful to represent and visualize a complexity of interactions of items interested (Diebold and Yilmaz, 2014). A graph is comprised of a series nodes/vertices and the edges, referring to connect or join two nodes  $i, j$ . In this study, each node is represented as a particular SIFI, while the edge between two nodes indicates their dependence. The properties of a graph can be expressed by its adjacency matrix  $A$ , a square matrix comprising the elements of  $a_{ij}$  with value equal to one if an edge connects to node  $i$  and  $j$  and zero otherwise. In social networks such as Facebook or Twitter, a friendship can be naturally defined or it could be a follower-followee relationship. However, for institutional networks, defining an adjacency matrix is not as intuitive or trivial as what can be done in individual networks. We may need additional prior knowledge regarding counterparty linkages such as their contractual obligations, interbank lending and the assets they hold mutually, which are relatively hard to be gathered in time and are indeed very low-frequent data type. Therefore, Diebold and Yilmaz (2014) use daily stock returns for its forward-looking assessment advantage and being able to reflect the health of SIFI in time, accordingly they propose a variance decomposition matrix of volatility as an adjacency matrix. Concentration on volatility falls short though on quantifying the dynamics of tail event related measures.

This study therefore constructs an adjacency matrix from risk profiles. The risk profile includes not only Implied Volatility (IV) but also tail risk measures such as Value-at-Risk (VaR) and Expected Shortfall (ES) to align with the Basel committee's definition on market risk. In addition, it is in accordance with the CoVaR concept of Adrian and Brunnermeier (2016), Härdle et al. (2016) and Hautsch et al. (2014). Compared with volatility, tail risk measures are more crisis-sensitive.

A pair of SIFIs is connected if their risk profiles share a certain degree of similarity. The similarity here is defined via a risk profile vector comprised of three risk covariates. More



Index	Name of SIFI	Firm Size	Debt Ratio	Bucket	Country
1	JP MORGAN CHASE	21.506	0.261	4	U.S.
2	BANK OF AMERICA	21.446	0.302	2	U.S.
3	BANK OF NEW YORK MELLON	19.499	0.095	1	U.S.
4	CITIGROUP	21.359	0.300	3	U.S.
5	GOLDMAN SACHS	20.624	0.509	2	U.S.
6	MORGAN STANLEY	20.501	0.417	2	U.S.
7	STATE STREET	19.106	0.153	1	U.S.
8	WELLS FARGO	20.980	0.183	1	U.S.
9	ROYAL BANK OF SCTL	21.588	0.252	1	U.K.
10	BARCLAYS	21.604	0.286	3	U.K.
11	HSBC	21.682	0.127	4	U.K.
12	STANDARD CHARTERED	20.136	0.187	1	U.K.
13	BNP PARIBAS	21.684	0.136	3	France
14	CREDIT AGRICOLE	21.489	0.211	1	France
15	SOCIETE GENERALE	21.184	0.139	1	France
16	DEUTSCHE BANK	21.630	0.200	3	Germany
17	UNICREDIT	20.929	0.360	1	Italy
18	ING GROEP	21.156	0.103	1	Netherlands
19	SANTANDER	21.158	0.368	1	Spain
20	NORDEA BANK	20.476	0.326	1	Sweden
21	CREDIT SUISSE GROUP N	20.744	0.339	2	Switzerland
22	UBS GROUP	21.008	0.251	1	Switzerland
23	BANK OF CHINA	21.200	0.160	1	China
24	ICBC	21.508	0.089	1	China
25	CHINA CON.BANK	21.281	0.092	1	China
26	MITSUBISHI UFJ	21.533	0.159	2	Japan
27	MIZUHO	21.247	0.233	1	Japan
28	SUMITOMO.MITSUI	21.044	0.125	1	Japan

Note: Debt ratio, a ratio of total debt to total asset, and bank size, as log value of total assets denominated in the US dollar, are shown as their mean value during sample period (2007-2015). The buckets assigned by BCBS correspond to required level of additional common equity loss absorbency as a percentage of risk-weighted assets from 3.5% (Bucket 5), 2.5%(Bucket 4), 2.0%(Bucket 3), 1.5%(Bucket 2) to 1%(Bucket 1).

Table 1: The overview of SIFIs

precisely, we calculate the cosine similarity at each time point  $t$ :

$$\rho_{ij,t} = \frac{X_{i,t}^\top X_{j,t}}{\|X_{i,t}\| \|X_{j,t}\|} \quad \text{for } j \neq i, \quad i = 1, \dots, N, \quad t = 1, \dots, T, \quad (1)$$

where  $X_{i,t} = [VaR_{i,t}, ES_{i,t}, IV_{i,t}]^\top$  is a risk profile vector in node  $i$  comprising its conditional VaR at 95% level, conditional ES at 95% level and average IV from options markets. The conditional VaR for each  $i$  is calculated by first regressing for each calendar year (starting 2007) the return vector of a fixed SIFI on the returns of the remaining SIFIs. In the second step one calculates the 5%-quantile of the residuals of this regression as conditional VaR for this specific calendar year. Having the conditional VaR estimated, one obtains the conditional ES as the mean value of residuals return lower than this conditional VaR. “Partialing out” the risk component of other SIFIs is in the spirit of Adrian and Brunnermeier (2016) and Chan-Lau et al. (2016) to represent the direct connection among SIFIs. The IV data of each SIFI is collected from Bloomberg at weekly frequency, and for each SIFI, its IV time series is regressed on the IV from the remaining SIFIs to get the residual IV. We then calculate the mean value of residual IV as one of risk covariates.

The risk profile similarity in (1) is analogous to the Pearson correlation coefficient, and is the dot (scalar or inner) product of the normalized and centered risk profile vectors. For any pair  $(i, j)$ , as long as the normalized risk vectors move to the same direction, the cosine of the angle between them shall be very small, therefore,  $\rho_{ij,t}$  will approach one (analogous to positive  $\Delta\text{CoVaR}$  or positive tail dependence). Likewise, moving to reverse directions will result in a larger angle and a smaller or even negative  $\rho_{ij,t}$  if the angle is higher than  $\pi/2$  (analogous to negative  $\Delta\text{CoVaR}$  or negative tail dependence). The appealing feature is that it covers a wide range of tail and volatility risk, especially if the return distribution is not normal with higher moment components deviating from the normal moments.

Indeed if the data are jointly normal the tail risk is a function of volatility  $\sigma$  only since it upscales the standard normal quantiles  $q_\alpha$  to the VaR as  $\sigma q_\alpha$ . The same is true for  $ES = E(X|X > VaR)$  and for the implied volatility (see more discussion in Franke et al. (2015)). In essence: for a normal distribution the three elements of the risk profile are

(nonlinear) functions of each other. For the more realistic non-normal case we expect therefore a more precise fingerprint of the risk profile.

The cosine similarity in (1) is displayed in Figure 1. The colors used to represent the degree of similarity vary from negative (blue) to positive correlation (yellow) in the grids. We snapshot eight situations at 31.12 based on an annual interval from 2007 to 2014. Through 2007 to 2009, one observes the similarity moving to a wide coverage of yellow color to signal an increasing (decreasing) interdependence on positive (negative) side. During the severest time of system stress, most of financial institutions are tightly tail connected. As the tension for crisis has gradually decreased, one sees a reduced connectedness in 2010. The European debt crisis threatening the financial markets in 2013, therefore the resulting similarity matrix turns to more yellow again, especially for a clear yellow block shown in the European SIFIs (node 11-22). Figure 1 shows that the similarity matrix indeed varies over time. The incorporation of this dynamic effect is left for further research. To promptly capture an approximate dynamics of risk similarity, the covariates are estimated during a given window size, here we work with the length of window  $h = 90$  (roughly 1/3 of a year).

## 2.3 Adjacency matrix

It has to be understood though that the pairwise similarities do not reveal equal severity; some are profound but some are not. It is not advisable to take all pairwise similarities into account if they are not beyond a certain threshold, an observation also made by Härdle et al. (2016), Hautsch et al. (2014) and Barigozzi and Brownlees (2015). Therefore, to achieve manageable and interpretable structures, dimension reduction techniques are employed.

The simplest network structure is based on binary weights representing the links between the nodes, with one (zero) used to represent a link (isolation). Systemic risk, however, is induced by positive interdependencies, whereas the negative ones are benefiting a risk diversification. Thereby, the instability indeed is caused by positive rather than negative interdependence, suggesting an asymmetric impact. The necessity to treat positive and negative correlations (the entries of the similarity matrix) differently makes therefore

such a breakdown into a binary structure infeasible. Additional evidence for this fact provides Figure 3. Here we plot the fraction of positive correlations constituting the similarity matrices dynamically over time. The figure shows that during the 2008-2009 crisis period a extremely high cutoff correlation is necessary due to systemically strong interdependence during the crisis. Also in other periods we observe that the fraction of positive correlations is higher than 50%. Thus the positive and negative correlation cannot be treated in the same fashion. One needs to create more groups in order to disentangle positive and negative values.

Here we propose to partition the ordered correlations into three groups. In fact more groups would be possible, but simplicity of visualization and subsequent analysis in the TENQR model suggest that three groups seem to do the job here. Highly negative correlations indicate an adverse comovement of risk profiles. Highly positive similarities indicate strong interrelationship between the SIFIs, while the correlations close to zero reflect weak or no linkages. The assignment of the correlations to one of three groups is based on a classification technique. Algebraically, let  $\rho = (\rho_1, \rho_2, \dots, \rho_n)^\top$  to be the vector of ordered similarities and  $\rho_1 < \rho_2 < \dots < \rho_n$  where  $n = N(N-1)/2$ . Since the similarities between the risk profiles are frequently high, we apply Fisher's  $Z$  transformation:

$$\rho_j^* = \frac{1}{2} \log \left( \frac{1 + \rho_j}{1 - \rho_j} \right).$$

The transformed correlations are approximately normally distributed with the constant variance  $1/(h-3)$  where  $h$  is the sample size. This is different from the setup in Ng (2006), since we do not concentrate on zero vs. nonzero correlations only but also on the direction of correlation. The edges of the network are constructed based on large spacings between two subsequent correlations to indicate a large mean-shift in the original correlations or a slope shift in the transformed values:

$$\Delta_j = \Phi \left( \sqrt{h-3} \rho_j^* \right) - \Phi \left( \sqrt{h-3} \rho_{j-1}^* \right).$$

The objective is to split the sequence of spacings into three subsets using a classification approach. Let  $\theta_1$  be the fraction of spacings which corresponds to highly negative correlations and  $\theta_2$  be the fraction of spacings which separates highly positive correlations. A

global minimization of the total sum of squared residuals results in:

$$(\hat{\theta}_1, \hat{\theta}_2) = \underset{\theta_{1,2} \in [\underline{\theta}, \bar{\theta}]}{\operatorname{argmin}} \sum_{j=1}^{[\theta_1 n]} (\Delta_{(j)} - \bar{\Delta}_S)^2 + \sum_{j=[\theta_1 n]+1}^{[\theta_2 n]} (\Delta_{(j)} - \bar{\Delta}_M)^2 + \sum_{j=[\theta_2 n]+1}^n (\Delta_{(j)} - \bar{\Delta}_L)^2$$

and

$$\begin{aligned} \bar{\Delta}_S &= \frac{1}{[\theta_1 n]} \sum_{j=1}^{[\theta_1 n]} \Delta_{(j)}, \\ \bar{\Delta}_M &= \frac{1}{[\theta_2 n] - [\theta_1 n]} \sum_{j=[\theta_1 n]+1}^{[\theta_2 n]} \Delta_{(j)}, \\ \bar{\Delta}_L &= \frac{1}{n - [\theta_2 n]} \sum_{j=[\theta_2 n]+1}^n \Delta_{(j)}, \end{aligned}$$

where  $\Delta_{(j)}$  are ordered spacings and  $[\theta n]$  is the integer part of  $\theta n$ . We have taken  $\underline{\theta} = 0.1 = 1 - \bar{\theta}$  and found stable results for this choice. We obtain the optimal break fractions  $(\hat{\theta}_1, \hat{\theta}_2)$  resulting in a minimum total sum of variances from three subgroups to make the correlations in a given group as homogeneous as possible. Alternatively we applied a  $k$ -means classification and found similar allocations.

Having estimated the break fractions  $\theta_1, \theta_2$  at each time point, we classify the similarities into three groups. The 1st group contains pairs of SIFIs with a very strong positive dependence. The corresponding cells of the adjacency matrix are coded with ones indicating active links and shown as a white grid in Figure 2, i.e.  $a_{ij} = a_h$  standing for high positive correlations. The elements of the adjacency matrix for the 2nd group are set to  $a_m$  reflecting weak or inactive linkages and a black grid in Figure 2. Finally, the 3rd group contains pairs with high negative correlation and is coded with  $a_\ell$  and shown as a gray grid. Thus distinguishing between direct comovement of risk measures, uncertain comovement and adverse comovement. The pairwise and symmetric  $a_{j,i}$  are the elements in the adjacency matrices  $A$ .

The value  $a_h = 1$  reflects a strong comovement and  $a_m = 0$  the weak links. Finally,  $a_\ell$  should satisfy  $a_m < a_\ell < a_h$ , so this is set to  $a_\ell = 0.5$  to reflect an asymmetric impact in a network system. Other choices of the weights less than one are possible too, but again the presented results turned out to be stable with respect to the choice of the weights. Note that a directed graph is not an option in this framework, since the simple correlations do

not reveal the causal dependence needed for a directed network. Unless the availability of interbank relationship, estimating  $A$  is required in the following TENQR model and makes network structure feasible and flexible, in comparison with a given  $A$  in the work of Zhu et al. (2016).

## 2.4 Systemic risk score and risk decomposition

In social networks one might consider nodes/persons with many connections to be important or central. In the case that we study here, though we like to identify nodes as central as they being likely to contribute the most to systemic risk. It may be informative for the supervisory authority for deciding capital requirements and systemic risk charges to corresponding SIFIs, see Table 2. The systemic risk scores over years quantify the degree of systemic risk in the financial system to give an earlier warning signal for policy makers. The afterward risk decomposition tool conveys the information of the risk contribution of each SIFIs, which can be ideally regarded as a complement of the bucket approach proposed by Basel Committee on Banking Supervision (BCBS).

In addition to the notion of interconnectedness, node characteristics, e.g. size of bank or risk level of bank are also decisive and shall be considered. A bank with bigger market capitalization is more capable of offering interbank loans to other financial institutions, describing the situation of “too-big-to-fail”. It’s understood that risk in a connected network is provoked by either the compromise level of nodes or the degree of their connectedness, or even both. Das (2016) proposes a parsimonious and intuitive metric for quantifying aggregate risk in a network comprised of related entities, and also for decomposing the relative risk contribution of each node on the aggregate network risk.

The adjacency matrix,  $A$ , in Figure 2 plays a major role in these two analyses. The compromise level of nodes is the risk vector for all nodes, one can define this risk vector e.g. the size of node, the capital allocation on each node (like the weights of a portfolio) or nodal characteristics used to measure the nodal risk (e.g. debt ratio, credit rating, probability of default, etc.). Referring to the issue of too-big-to-fail and Basel III regulation, we define the level of compromises as nodal market capitalization, and have a compromise vector  $C = (C_1, \dots, C_N)^\top \in \mathbb{R}^N$ . The systemic risk score,  $S$ , as a scalar is

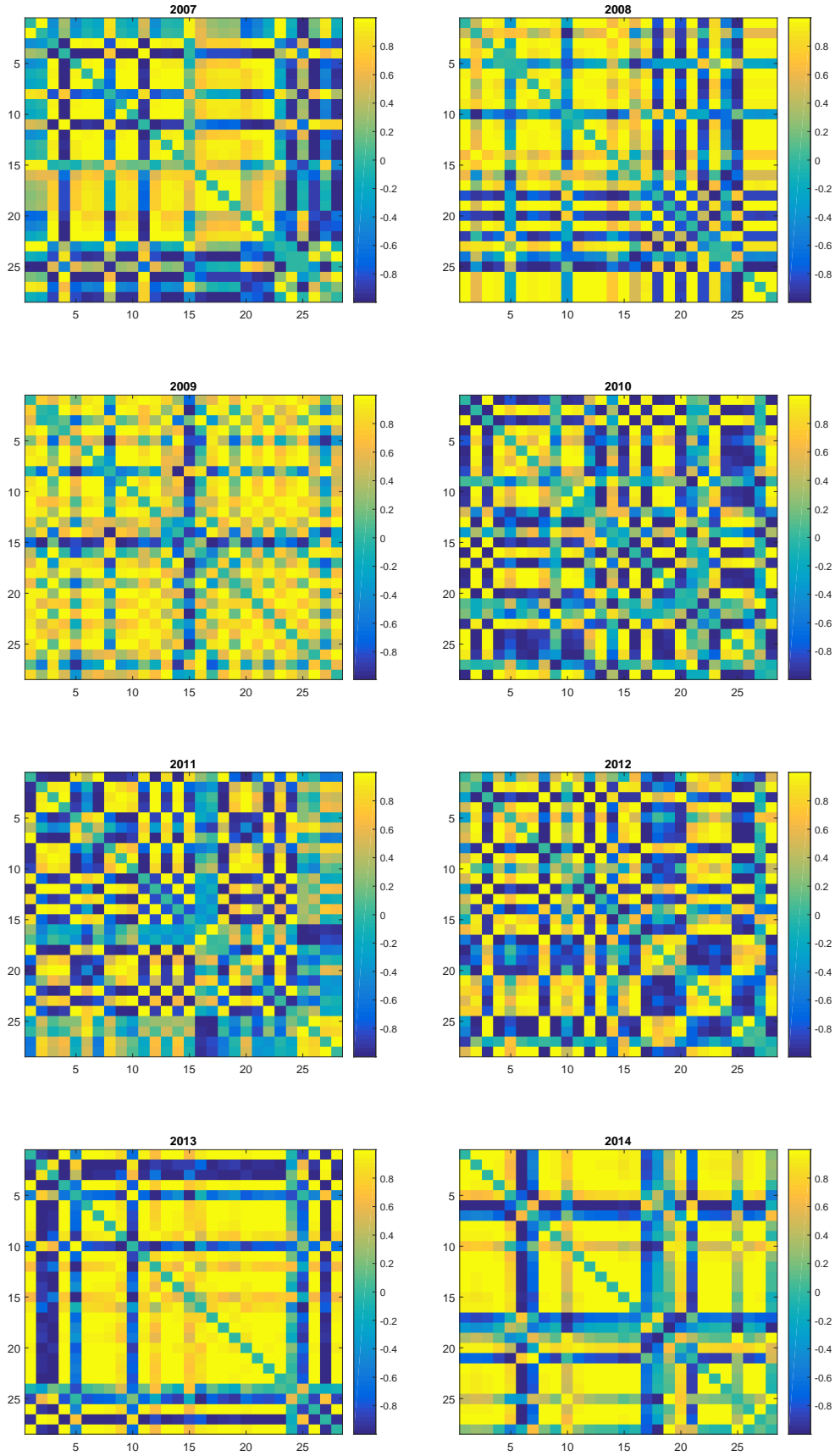


Figure 1: Similarity matrix

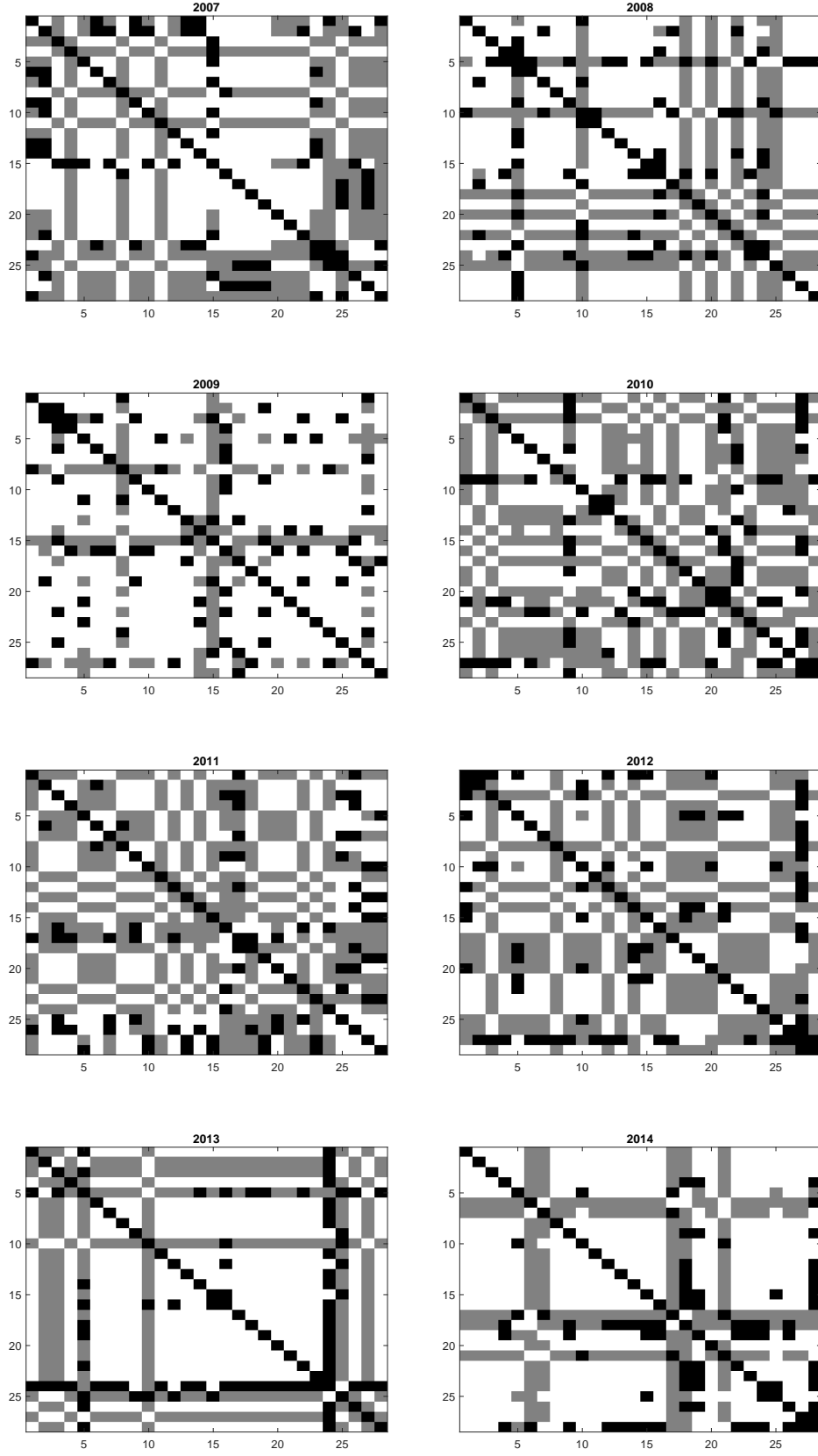


Figure 2: Adjacency Matrix

Note: the highly positive correlation (in white), the highly negative correlation (in gray) and the weak correlation (in black) are shown in each of calendar years. The diagonal cells show a trivial relation and in black as a default color.



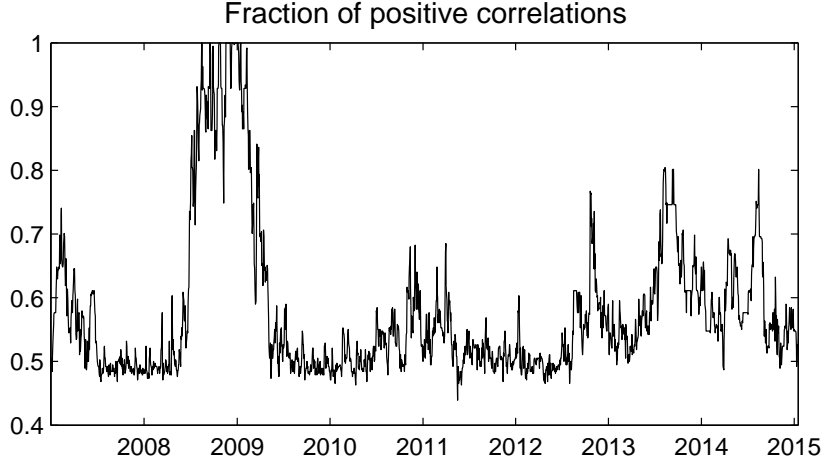


Figure 3: Fraction of positive correlations in the similarity matrix

the function of the compromise level for all nodes and the connectedness defined by the adjacency matrix  $A$ :

$$S(C, A) = C^\top AC \quad (2)$$

The systemic risk score,  $S(C, A)$ , will be very useful in ensuing analytic e.g. risk decomposition technique.

By definition, the risk decomposition technique decomposes the aggregate risk score into individual risk scores to reflect nodal risk contribution  $S_i$ , such that  $S = \sum_{i=1}^N S_i$ . Due to that the function  $S(C, A)$  is linear homogeneous in the risk vector  $C$ , this idea can be easily carried out by applying the Euler's equation that decomposes first-order homogeneous functions:

$$S = \sum_{i=1}^N S_i = \frac{\partial S}{\partial C_1} C_1 + \frac{\partial S}{\partial C_2} C_2 + \cdots + \frac{\partial S}{\partial C_N} C_N \quad (3)$$

Through Euler's rule, the aggregate systemic risk score is manageable by ranking nodal risk contributions. One can focus on the nodes with relative higher risk contributions arising from its connectedness,  $\frac{\partial S}{\partial C_i}$ , or from the risk level  $C_i$ . For a regulatory purpose, the node with a wide range of connectedness shall be prioritized and supervised as it has

higher risk increment. In a nutshell, this analytic decomposition enables identifying the source of systemic vulnerabilities.

Table 2 summarizes the results of risk decomposition of each node on annual basis ranging from 2007 to 2015. The aggregate systemic risk score rises subject to the outbreak of the US subprime crisis and lasts until end of 2009. As expected, the US SIFIs on average since 2008 contribute the highest systemic risk into the global systemic risk. The aggregate risk score is an ideal measure to quantify systemic risk. Systemic risk is not easy to define, but the universally accepted characteristics are that it has large impact, and is widespread, and has a ripple effect that endangers the financial system. One can find a dramatic rise in risk score in 2008, indicating that a potential systemic risk emerges w.r.t the aforementioned characteristics. The systemic risk remained high until 2009 and declined in 2010 to the historically lowest point to signal the resilient global economy and effective monetary policies after crisis. In 2013 during the European debt crisis, one sees that the European SIFIs (nodes 9-22) suffered in terms of their higher systemic risk contributions. The aggregate systemic risk score increased again and lasted until 2015 as the consequence of the Chinese stock market crash in summer 2015 caused by insolvent shadow banks, bursting asset bubbles and indebted local governments.

It is worthwhile to highlight the risk decomposition in relation to the notion of central nodes. The node with the highest risk contribution is then to be seen as the central node. Through equation (3), one may attribute the high risk node as the one with a greater magnitude of compromise or high interconnectedness, or both. Such critical nodes need immediate attention from regulators. One can e.g. find the node 11 (HSBC) as a central node in 2010, 2012, 2014 and 2015, while the node 1 (JP. Morgan) becomes a central hub in the 2008-2009 US subprime crisis. To validate the results, we compare the identified central SIFIs in this study with the SIFIs assigned to Bucket 4 (highest loss absorbency group) reported in FSB Nov. 2015. We observe that the risk decomposition analysis yields an almost identical list for this bucket.

A geographic analysis based on this table documents to which extent systemic risk is attributed to a particular region where the headquarters of SIFIs are located. Before 2014, the average scores in Europe are slightly larger than that of the US due to the fact that European banks build the majority of SIFIs. European banks are the largest geo-

graphic group within the 50 biggest global banks (21 banks from eight different European countries), while the US only contributes 7 banks. The contribution from the US region is getting higher after 2014, which may be caused by an increased connectedness between this region and others as shown in Figure 1. To underscore this point, in the aftermath of the US subprime crisis, meaningful M&A transactions were few as banks nursed their balance sheets, stock prices back to health, and the disciplines from regulators. In these recent years, many US banks pursue long-sought strategic consolidation. The urge to merge is the confluence of long history of low interest rate resulting in the lowest average net interest margin according to the FDIC (Federal Deposit Insurance Corporation) report, higher fixed regulatory costs and rapidly changing technological and financial innovation.

### 3 Tail event driven network quantile regression

The previous section provided a descriptive analysis of the SIFI and quantified the connectedness via an adjacency matrix. In this section we present three issues on the network dynamics. First, it is of interest to relate the response of individual node at a given time point to the quantified connectedness at the previous time point. Second, it's very likely that the return of individual SIFI asymmetrically response the network factor, that is, the node responses strongly to the network factor when it is under a stress (extremely negative returns) but may react mildly when it is experiencing an advance. The likelihood of simultaneous slumps in the banking industry is potentially greater than that they boom together, which is a typical feature under systemic risk. Diebold and Yilmaz (2014) and Xu et al. (2016) find an increased total interconnectedness during the crisis period, resulting in more fragile financial markets evidence by high comovement, contagion and spillover. By investigating global banking sectors, Dungey and Gajurel (2015) find a systematic contagion, defined as the potential increased exposure of banks to total systemic risk, rises in a crisis. Similar findings but through different connectedness measures are by Adrian and Brunnermeier (2016) and Hautsch et al. (2014). Recalling that systemic risk is defined through (i) large impact, particular in the downside constituting an asymmetric reaction; (ii) widespread coverage that can be examined through a panel

	SIFI	2007	2008	2009	2010	2011	2012	2013	2014	2015
1	JP MORGAN	150	217	221	153	158	150	205	225	205
2	BANK OF AMERICA	135	193	207	172	186	172	140	223	149
3	BANK OF NEW YORK MELLON	171	187	149	138	149	138	121	206	64
4	CITIGROUP	158	193	210	171	175	189	207	199	202
5	GOLDMAN SACHS	182	83	168	178	161	152	87	192	187
6	MORGAN STANLEY	175	197	202	160	164	182	200	130	191
7	STATE STREET	164	176	190	160	138	171	188	132	180
8	WELLS FARGO	159	207	149	181	182	156	206	221	193
9	ROYAL BANK OF SCTL	191	201	204	109	168	190	211	198	198
10	BARCLAYS	190	107	219	182	173	160	131	214	204
11	HSBC	171	212	220	187	173	192	210	226	211
12	STANDARD CHARTERED	179	196	208	152	167	141	193	200	121
13	BNP PARIBAS	178	200	211	160	161	190	209	211	155
14	CREDIT AGRICOLE	181	194	183	171	182	142	207	214	130
15	SOCIETE GENERALE	146	188	115	151	162	168	205	193	202
16	DEUTSCHE BANK	202	160	155	169	142	192	182	202	150
17	UNICREDIT	199	199	189	167	110	159	208	119	202
18	ING GROEP	196	125	221	169	156	147	202	85	197
19	SANTANDER	202	216	183	183	174	155	204	155	194
20	NORDEA BANK	191	125	215	154	163	150	202	217	93
21	CREDIT SUISSE GROUP N	193	206	218	117	179	170	205	133	193
22	UBS GROUP	182	129	199	134	156	184	201	198	147
23	BANK OF CHINA	143	185	209	172	166	183	200	193	173
24	ICBC	131	105	212	148	162	188	43	185	197
25	CHINA CON.BANK	151	139	198	149	161	151	114	203	196
26	MITSUBISHI UFJ	148	206	216	163	142	160	206	201	209
27	MIZUHO	146	204	147	103	153	69	140	211	205
28	SUMITOMO.MITSUI	131	201	215	168	148	189	202	111	196
	Systemic Risk Score	4746	4938	5430	4419	4514	4588	5032	5193	4942
	Average score (US)	162	182	187	164	164	164	169	191	172
	Average score (Europe)	186	175	196	157	162	167	198	183	171
	Average score (Asia)	142	173	200	150	155	157	151	184	196

Table 2: Systemic risk decomposition

or stack model; (iii) a ripple effect being detected by an intertemporal investigation, the TENQR model is proposed for accommodating three definitions. This aspect is beyond the work of Zhu et al. (2016) who focus on the asymptotics of the involved parameters.

Third, for financial assets, it's very likely that their returns are subject to the impact of neighboring assets in the sample industry or geographic region. Modelling residuals for each asset individually revealed, as we show in the next section interesting insights into the common behavior of assets from the same geographic region (see Brechmann et al. (2013)). For this reason we consider the pooled quantile regressions for the SIFIs from the US, Europe and Asia. By doing so, one may know which region is more vulnerable with the network factor. With this understanding, the impact caused by a systemic network is likely to be region-specific.

In a nutshell, the extant research overwhelmingly using the VAR framework requires ex-post analysis of the network structure and may fail because of curse of dimensionality. This motivates a parsimonious model which incorporates tail sensitivity, allows for an asymmetric impact, establishes an intertemporal framework for investigating a ripple effect and evaluates regional reactions on network risk and the corresponding impulse response for the network shocks.

### 3.1 TENQR model

For the aforementioned purposes, we pay particular attention to tail events, like extremes or high level quantiles. A convenient framework which serves these two objectives is the quantile autoregression model of Koenker and Xiao (2006). It yields insight into the interrelation of the involved risk factors, and allows the investigator to explore a range of conditional quantile functions that links the dependent variable and the covariates in a continuous and smooth manner. However, this triggers problems if the number of nodes increases, and it happens if one would like to estimate the VaR/CoVaR via quantile regression. Using an index mimicking the financial system Adrian and Brunnermeier (2016) is an alternative solution, though it is simple but lacks a network insight. Besides, the network in the financial system is time-varying with different degree of interconnectedness over time. To tackle this we introduce a network factor involving the adjacency matrix

as proposed in Zhu et al. (2017) and Zhu et al. (2016) to represent the financial system in a more practical way.

We first opt for a quantile regression for the pooled residuals from (4) with the explanatory variables given by the proposed network factor. For each node  $i$  at time  $t$  we denote the return by  $Y_{it}$ . The SIFI dynamics is first approximated by:

$$Y_{it} = \alpha_0 + \alpha_{i1}Y_{i,t-1} + \alpha_{i2}^\top W_t + \alpha_{i3}^\top S_{it} + v_{it}, \quad \text{for } i = 1, \dots, N, \quad t = 1, \dots, T \quad (4)$$

where  $Y_{i,t-1}$  is the autoregressive term and accounts for persistence and missing variables.  $W_t$  represents the market-wide covariates used to capture systematic factors, while  $S_{it}$  stands for node-specific characteristics. Equation 4 is estimated using simple OLS either for each node individually or in a stacked form for groups of nodes. Two market-wide factors, namely the volatility index VIX proxied for the perceived market sentiment and the TED rate proxied for perceived credit risk are chosen. The node-specific variables are the log firm size and the debt ratio computed as the total debt to assets ratio. Practically, large and well-capitalized banks are more likely to issue interbank loans to a large body of counterparties, creating more interconnected interbank relationship. In this sense, their returns relative to those of smaller SIFIs are bounded by this special treatment. The debt ratio, namely leverage ratio, is an indicator for the tendency of financial distress. All measures are denominated in USD.

The residuals,  $\hat{v}_{it}$ , from (4) can be seen as “residual returns” corrected for indirect impact from the market-wide covariates, persistence and nodal characteristics. The network effect may account for the missing covariates shown in (4), in other words, these residuals may contain information on the network. The sets  $\mathcal{R}_r$  with  $r = 1, 2, 3$  contain the  $i$ -indices of SIFIs for each of the regions US, Europe, and Asia. The random coefficients model which is a building block for the quantile regression is

$$\hat{v}_{it} = \beta_{r0}(U_t) + \beta_{r1}(U_t) \sum_{j \in B_i} m_i(Y_{j,t-1}) \quad \text{for } i \in \mathcal{R}_r. \quad (5)$$

The coefficients  $\beta_{rp}(U_t)$  for  $p = 0, 1$  are unknown function mappings  $[0, 1] \rightarrow \mathbb{R}$ ,  $B_i$  is a set of neighboring nodes for node  $j$ , and  $m_i(Y_{j,t-1})$  is a function of the neighboring nodes of node  $i$ . Furthermore,  $\{U_t\}$  is a sequence of iid standard uniform random variables. In

terms of the above objectives  $\beta_{r1}$  stands for the network effect. Since if the right hand side of (5) is monotonous in  $U_t$ , we can state the conditional quantile function of  $\hat{v}_{it}$  as

$$Q_{\hat{v}_{it}}(\tau|\mathcal{I}_{t-1}) = \beta_{r0}(\tau) + \beta_{r1}(\tau) \sum_{j \in B_j} m_i(Y_{j,t-1}) \quad \text{for } i \in \mathcal{R}_r, \quad (6)$$

where  $\mathcal{I}_{t-1}$  denotes the information on all SIFIs observable at  $t-1$ . The coefficients depend on  $\tau$  and allow for different impacts of the corresponding covariates on the quantiles of the response variable. Functions  $m_i(Y_{j,t-1})$  quantify the connectedness of the nodes within the network and we use the adjacency matrix to aggregate the network impact

$$\sum_{j \in B_i} m_i(Y_{j,t-1}) = \frac{1}{|B_i|} \sum_{j=1}^N a_{ij,t-1} Y_{j,t-1}. \quad (7)$$

Equation (7) measures the average impact from  $i$ -th node neighbors and can be interpreted as “network factor”. The network factor quantifies the average of its connected neighbors for each node in the system, which may contribute to the return prediction for the next day. Besides, this approach has clear advantages compared to full vector (quantile)-regressions: in large networks the number of the unknown parameters may exceed the number of observations. The extension to time-varying parameters is technically demanding and requires specific assumptions on the data generating process. In the setup advocated here we estimate the relationships within the network exogenously and treat the elements of the adjacency matrix as given. For notational convenience we collect the two parameters for each region  $r$  in vector  $\theta_r(\tau) \in \mathbb{R}^2$ , i.e.  $\theta_r(\tau) = \{\beta_{r0}(\tau), \beta_{r1}(\tau)\}$ . The estimation follows by minimizing the objective function as in Koenker and Xiao (2006):

$$\hat{V}_r(\tau) = \min_{\theta_r(\tau) \in \mathbb{R}^2} \sum_{t=1}^T \sum_{i \in \mathcal{R}_r} \rho_\tau \left\{ \hat{v}_{it} - \mathbf{x}_{i,t-1}^\top \theta_r(\tau) \right\} \quad \text{for } \tau \in (0, 1). \quad (8)$$

Here  $\rho_\tau(u) = u \cdot \{\tau - I(u < 0)\}$  is an asymmetric loss function and  $\mathbf{x}_{i,t-1}^\top$  collects all relevant explanatory variables. We denote the solution of the optimization problem with  $\hat{\theta}_r(\tau)$ . Algorithms to solve (8) can be found on <http://www.quantlet.de> and in Tran et al. (2016). The conditional quantile of  $\hat{v}_{it}$  can be estimated by  $\hat{Q}_{\hat{v}_{it}}(\tau|\mathcal{I}_{t-1}) = \mathbf{x}_{i,t-1}^\top \hat{\theta}_r(\tau)$  for an appropriate value of  $r = 1, 2, 3$ . Note that the individual and the pooled models do satisfy the assumptions of the standard quantile regression and we can rely on the

classical asymptotic theory. We do not take into account the estimation error in the residuals and treat these as given quantities.

The slope function of the estimated quantile regression is of key interest for the evaluation of the network effects. For the purpose of statistical inference we summarize the asymptotic properties of the estimator. Following, for example, Koenker and Bassett (1978) we obtain for each region in  $\mathcal{R}_r$ :

$$\sqrt{T|\mathcal{R}_r|}d_0^{-1/2}d_1\{\hat{\beta}_{r1}(\tau) - \beta_{r1}(\tau)\} \sim N(0, \tau(1 - \tau)),$$

with

$$d_0 = \lim_{T \rightarrow \infty} (T|\mathcal{R}_r|)^{-1} \sum_{t=1}^T \sum_{i \in \mathcal{R}_r} x_{i1,t-1}^2$$

$$d_1 = \lim_{T \rightarrow \infty} (T|\mathcal{R}_r|)^{-1} \sum_{t=1}^T \sum_{i \in \mathcal{R}_r} [f_i\{F_i^{-1}(\tau)\}] x_{i1,t-1}^2.$$

This holds assuming that (a)  $F_i$  have continuous density  $f_i\{F_i^{-1}(\tau)\}$  bounded away from zero and infinity near  $\tau$  for all  $r$ ; (b)  $d_0$  and  $d_1$  exist and are finite. We choose a specification which postulates a homoscedastic model for observations stemming from a single SIFI, but heteroscedastic if we move from one SIFI to another. The final estimator of the variance is of sandwich-type. Estimation of the nuisance parameter  $f_i\{F_i^{-1}(\tau)\}$  was heavily tackled in the literature and discussed in details, for example, in Koenker (2005). Here we opt for the Hendricks-Koenker estimator

$$\hat{f}_i\{F_i^{-1}(\tau)\} = T^{-1} \sum_{t=1}^T \frac{2h_T}{\mathbf{x}_{i,t-1}^\top \{\theta_r(\tau + h_T) - \theta_r(\tau - h_T)\}} \longrightarrow f_i\{F_i^{-1}(\tau)\} \quad \text{as } h_T \rightarrow 0.$$

The practical choice of the bandwidth can use the Gaussian approximation (Koenker (2005)).

For the purpose of inferences we employ the above asymptotic result in the Bahadur representation

$$\sqrt{T|\mathcal{R}_r|}d_0^{-1/2}d_1\{\hat{\beta}_{r1}(\tau) - \beta_{r1}(\tau)\}/\sqrt{\tau(1 - \tau)} \Rightarrow B(\tau) \quad \text{for } \tau \in (\epsilon, 1 - \epsilon),$$

where  $B(\tau) = W(\tau) - \tau W(1)$  is a one-dimensional Brownian bridge and  $W(\tau)$  is a



standard Brownian motion.

To evaluate the significance of the network factor consider the restricted variant of (8) with  $\hat{\beta}_{r1}(\tau) \equiv 0$ . Following Koenker and Machado (1999) we consider a Wald-type process with

$$\frac{T|\mathcal{R}_r|d_1^2}{\tau(1-\tau)d_0}\hat{\beta}_{r1}^2(\tau) \Rightarrow Q_{\eta(\tau)}^2(\tau) \quad \text{for} \quad \tau \in (\epsilon, 1-\epsilon),$$

where  $\eta(\tau) = \frac{T|\mathcal{R}_r|d_1}{\tau(1-\tau)d_0}\beta_{r1}^2(\tau)$  and  $Q_{\eta(\tau)}^2(\tau)$  is a noncentral version of the squared Bessel process with the noncentrality function  $\eta(\tau)$ . For fixed  $\tau$  this collapses to a noncentral  $\chi^2$  distribution with one degree of freedom. If the null hypothesis is that the network factor has no impact on the residual returns, we can use the above results to verify this hypothesis relying on

$$\sup_{\tau} \frac{T|\mathcal{R}_r|d_1^2}{\tau(1-\tau)d_0}\hat{\beta}_{r1}^2(\tau) \xrightarrow{\mathcal{L}} \sup_{\tau} Q^2(\tau),$$

with  $Q^2(\tau) = |B(\tau)|/\sqrt{\tau(1-\tau)}$ . The quantiles of the term on the RHS can be found numerically or in Andrews (1993).

It is important to stress a variety of applications of the above statements. First, they allow us to test the significance of the network factor in the quantile regression framework. Second, we can construct uniform confidence bands for the quantile effect of the network and to assess its nonlinearity or deviations from an ordinary linear regression. Third, we can compare the difference between the quantile curves for different geographic regions more rigidly from statistical perspective.

### 3.2 Estimation results

To estimate the above model we collect daily data on the SIFIs returns for the period from 01.01.2007 till 31.12.2015. For the regression (4),  $W_t = (VIX_t, TED_t)$  is the market-wide vector comprising the VIX and the TED spread. The node-specific variables are the log firm size and the debt ratio computed as the total debt to assets ratio available at annual frequency. To integrate it into (4) we keep the annual value constant on every day during the corresponding calendar year. Both variables naturally reflect the stability and the

riskiness of each SIFI. All measures are denominated in USD.

	const	$Y_{t-1}$	VIX	TEDrate	assets	debt ratio
US	-0.0267	-0.0626***	-0.0221***	0.0485**	0.0030	-0.1108
Europe	1.2054	0.0485***	-0.0183***	0.0080	-0.0564	-0.0595
Asia	1.9158	0.0145	0.0023	-0.0973***	-0.0861	-0.2937

Table 3: Estimation results for pooled regressions of SIFI returns on lagged return, market- and node-specific covariates for each geographic region. \*\*\* and \*\* stand for 1% and 5% levels of significance.

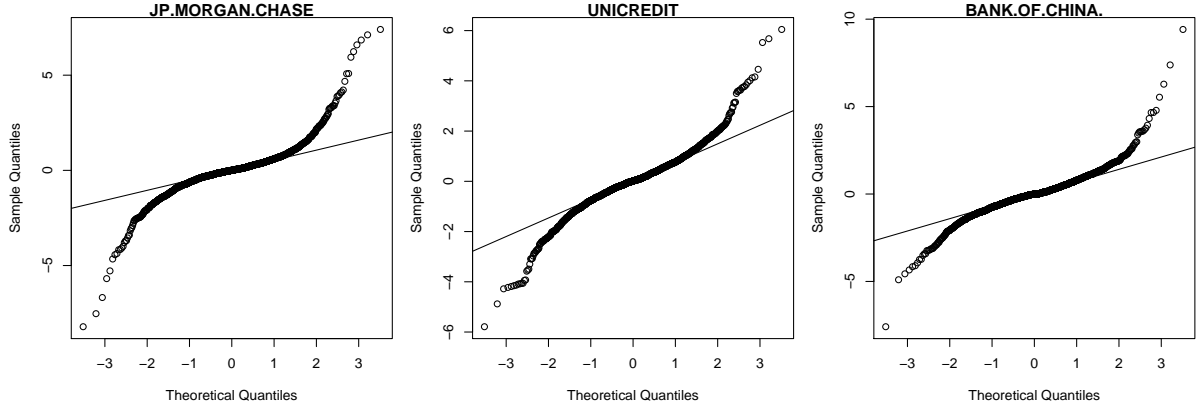


Figure 4: QQ plots of the absolute residuals from the individual regressions for JP Morgan, Unicredit and Bank of China and the Gaussian distribution (full sample estimation)

The residual returns  $\hat{v}_{it}$  from (4) exhibit heavy tails. Figure 4 shows as an example the normal QQ plots of the standardized residuals from the individual linear regressions for

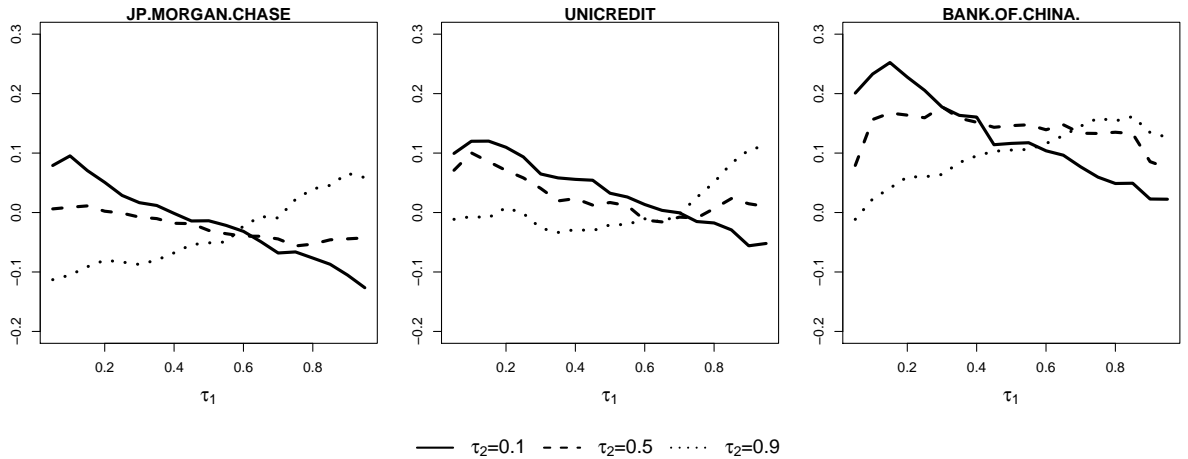


Figure 5: Quantilograms of residuals from the individual regressions 4 for JP Morgan, Unicredit and Bank of China with the 10%, 50% and 90% quantiles of network factor (full sample estimation)

JP Morgan (in the US), Bank of China (in Asia) and Unicredit (in Europe). We conclude that we have to deal with a heavy tailed distribution, suggesting a modeling approach with a focus on the tails. To assess the relationship between these extreme residuals and the network factor we consider the cross-quantilogram suggested by Han et al. (2016) equation (2). Therefore we consider the first order cross-quantilogram between  $\hat{v}_{it}$  and the network factor based on the full set of the SIFIs. Figure 5 shows the correlation of different quantiles of the residual returns for JP Morgan, Bank of China and Unicredit with the 10%, 50% and 90% quantiles of the network factor defined in (7). Since the curve for  $\tau_2 = 0.5$  is almost flat, JP Morgan is indifferent to neutral news from the market. The reaction to other network quantiles is higher for the 90%-quantile compared to the 10%-quantile. Unicredit rarely reacts to good shocks from the network factor in its turbulent times (low quantiles). Neutral news are, however, treated as negative shocks since the 50% and 10% quantile curves are very close. For Bank of China (BOC) all correlations are shifted upward, implying stronger sensitivity of the Asian companies to the network.

We provide the estimation results for the pooled regressions by grouping the SIFIs w.r.t their geographic origins. More specifically, we stack the returns and covariates of the SIFIs within each region together and estimate the resulting joint model. Furthermore, to model the causal impact of the network factor on the residuals we fit the quantile regression for each region as described in the previous section. The network factor takes all SIFI companies into account, but the dependent variable contains information only on SIFIs from a given region. Note that our interest focuses on the effect of the predictor, namely network factor, on the tails of residual return distribution, and compare the sensitivity or predictability of it at multiple percentiles. For this purpose, we resolve (8) separately for each of the  $q$  desired quantile levels,  $\tau_1 < \dots < \tau_q$ , to get  $\hat{\beta}_{1r}(\tau) = (\hat{\beta}_{1r}(\tau_1), \dots, \hat{\beta}_{1r}(\tau_q))$ . As can be seen in Figure 6, the predictability attributed to network factor varies with the quantile levels presenting a downward, upward or U-shape coefficient curve and the regions where the headquarters of SIFIs are located to demonstrate geographic distinctions regarding the structure of financial system.

For Asia, one sees a U-shape coefficient curve w.r.t desired quantile levels, whereas the European and the US SIFIs exhibit a monotonic coefficient curve. In addition, the Asian SIFIs exhibit the highest sensitivity to the network factor among the three regions. What

is very peculiar for these SIFIs is that the extent of sensitivity is almost the same for positive and negative shocks coming the network. Thus a high positive network factor induces positive shocks of the same magnitude as a high negative factor can provoke. Asian banks built up their borrowing from the international interbank market in the early 1990s, suffered though in the Asian Crisis (1997-1998). At that time, foreign banks curtailed their lending to Asian banks as evidence accumulated of their deteriorating loan quality. Since 2002, Asian banks have again begun to increase their borrowing from banks abroad and reached a peak of borrowing by 2006 before the US crisis (McCauley and Zukunft, 2008). The vulnerability of Asian SIFIs may therefore be caused by a curtailment of funding in the international interbank market, e.g. the US banks withdrawing the funding during the US subprime crisis and the European banks being forced to reduce their lending during the European debt crisis. Asian banks tend to suffer from global bank liquidity and credit crunches, on the other hand, they may gain from an improving function of global banking system, forming a U-shape coefficient curve in the Asian case.

A monotonically downward curve shown in the US and Europe indicates an asymmetric response to the network factor, namely a high negative network factor induces more profound negative shocks than the same magnitude of positive factor can provoke. The asymmetric impact of the network factor is in line with a number of research with a focus on crisis. The joint evidence of comovement, contagion and spillover is ascribed to an increased total interconnectedness in a financial system. See more discussion in Dungey and Gajurel (2015) and Diebold and Yilmaz (2014). It's worthwhile to note that our proposed quantile-varying estimators not only link bank returns and the global interbank network in a continuous and smooth manner but also avoid a dichotomous design (e.g. negative returns v.s. positive returns, crisis v.s. non-crisis period, lower volatility v.s. higher volatility) used in previous studies.

The 95% confidence bands in Figure 6 reveal several important facts. First, the impact of the network factor significantly differs from one geographic region to another. Thus the interpretation in the above paragraphs is statistically supported. Second, the zero value is not covered by the confidence bands indicating a significant impact factor. The horizontal lines visualize the slope parameter of a simple linear regression of residual returns on the network factor. Since the bands do not cover the constant coefficients,

it can be inferred that the variation in the quantile curves is again significant. Thus we conclude that the use of quantile regression is justified and shows statistically significant results.

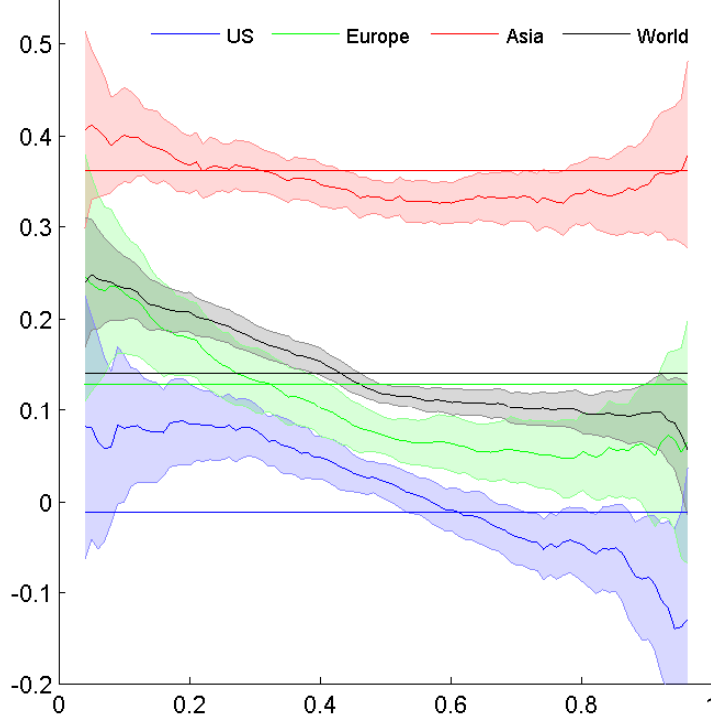


Figure 6: Slopes from the quantile regressions of the residuals from different geographic regions on the network factor (full sample estimation). The coloured area shows the 95% confidence band. The horizontal lines depict the parameters of the corresponding linear regressions.

To assess the time variation of the coefficient curves we perform a moving window estimation of the regional quantile regression with a 90-day window size. The resulting surfaces are shown in Figure 7. The surfaces for each region is comprised of the curves in Figure 6 estimated at each time point, in other words, they summarize the variation of quantile curves over time. In the Asian surface, one observes a high level of curves during the US crisis but the curves turn to slump afterward. The U-shape alike curves are evenly distributed over time but become more concave during the outbreak of turbulent episodes. For the US case, one rather observes a monotonic shape of curve from higher to lower quantile values in the majority of sample period. The US SIFIs trigger and transmit

credit crunch to one of the European or Asian counterparties, through the counterparties outside of the US the risk spreads widely and even amplifies in Europe and Asia in 2009. That may explain a stronger reaction in Asia and Europe in 2008-2009. Besides, a relatively bigger bank size in Asia and Europe renders a high risk level (“too-big-to-fail”), as a consequence, these banks account for most of systemic risk. The downward curves from lower to upper quantile are very promising in 2014, presenting a spike alike in the lower quantiles. To tease it out, one can refer to Table 2 again where the US region contributes the most in 2014. If some nodes are suffering, their regional neighbors will be infected observed by the adjacency matrix. Not surprisingly, the US SIFIs’ returns will react to this connectedness. Also, the European SIFIs react strongly and asymmetrically during the outbreak of European debt crisis. By focusing on the surface at 10% quantile, it appears that it varies with market turbulence or systemic tension accordingly.

In a nutshell, the TENQR method documents the importance of a network factor on the tail distribution and addresses an asymmetric response w.r.t the network factor. An investigation by moving window estimation visualizes the surface comprised of time-varying coefficient curves derived from quantile regression, indicating that the network factor contributes to return predictability a lot in economic downturn but less in the rest of periods. The implied vulnerabilities across regions are in accordance with the results of systemic risk decomposition. Having these efforts, we contribute to a “manageable” systemic risk. The supervisors are able to identify the central SIFIs with higher risk contributions, to measure the resulting connectedness in a system, and to evaluate the impact of network on the conditional quantile of a response.

## 4 Conclusion

There is no doubt that systemic risk depends on the interdependence and the joint dynamics of SIFIs in stress situations. The simultaneous stress on the financial system is proposed to be modeled in a network topology. The possible overstretching of positions i.e. the likeliness of common tail events is addressed in a quantile regression framework. The choice of the adjacency matrix is based on a similarity measure of a risk profile. This risk profile is composed of conditional VaR and ES (given the returns of other SIFIs)

together with the reported IV. The graph adjacency matrix is calculated from this similarity matrix by using a Fisher  $Z$ -transform based classification algorithm. Finally we fit the TENQR model to capture risk propagation and autoregressive network effect. The network geometry allows us to identify the risk contribution and the dominant risk contributors.

The network coefficient is analyzed regionally. In Asia, one obtains a U-shape curve (as a function of  $\tau$ , the stress level). The EU and US SIFIs show a monotonic shape but all exhibit the same sensitivity to the network factor. The Asian region though reacts to a high positive network factor with a positive shock, and also reacts to negative shocks coming from a negative network factor. This may be attributed to the lending policy in the early of 1980's follows by the Asian crisis 1997-1998. In summary, the TENQR model lets us isolate a network factor and thereby allows us to study the joint dynamics in a stress situation of the financial system. The implied vulnerabilities across SIFIs and regions are calculated via a risk decomposition analysis. The network topology of simultaneous events provides precise insight into the management of systemic risk. Supervisors may identify central SIFIs with higher risk contributions and predict their impact in the interconnected financial system.

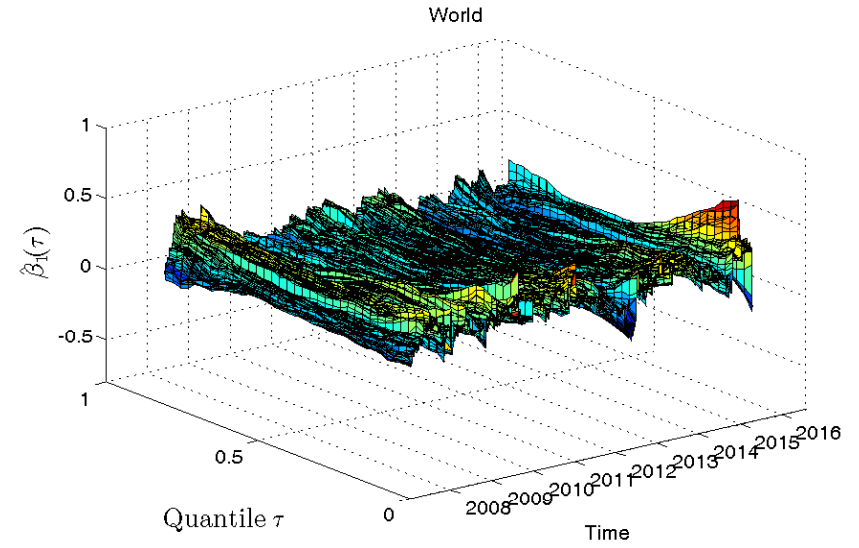
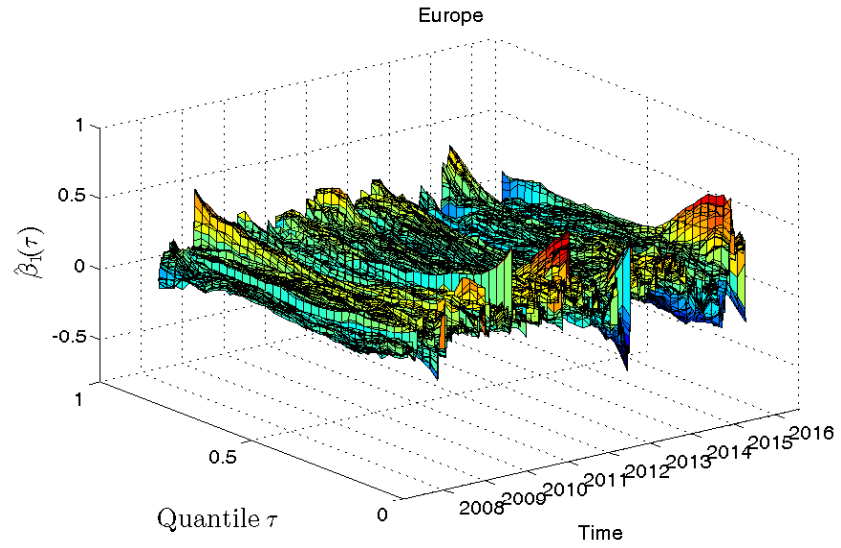
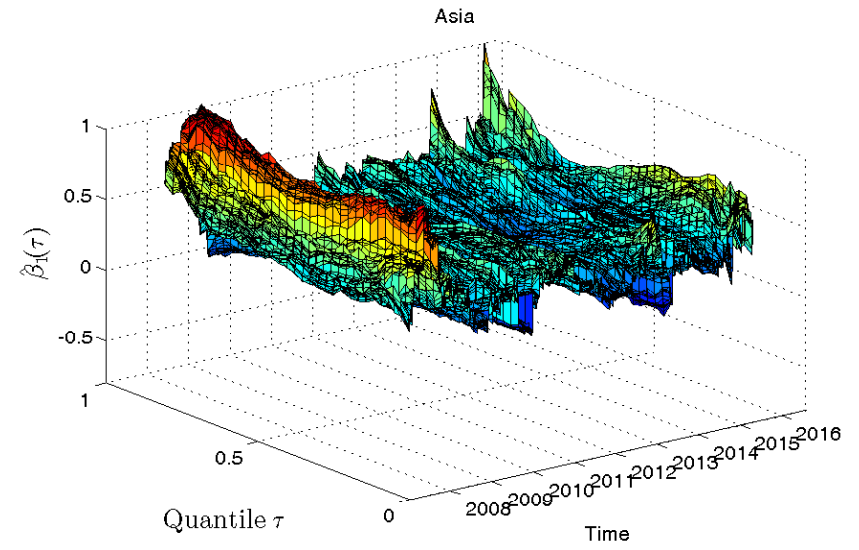
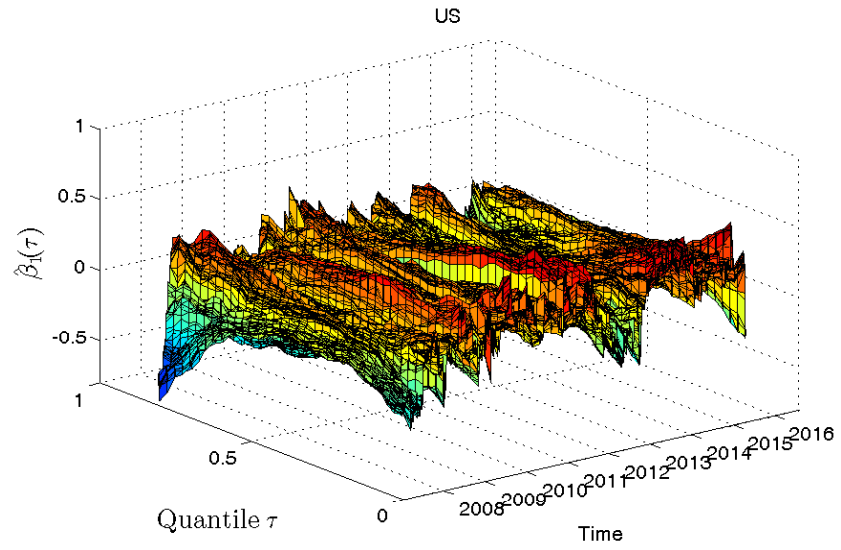


Figure 7: Moving window estimation of  $\beta_1(\tau)$  in the quantile regression (6) for the three geographic regions using the last 90 observations.



## References

- Adrian, T. and Brunnermeier, M. K. (2016). CoVaR, *American Economic Review* **106**: 1705–1741.
- Andrews, D. (1993). Tests for parameter instability and structural change with unknown change point, *Econometrica* **61**(4): 821–856.
- Barigozzi, M. and Brownlees, C. T. (2015). NETS: network estimation for time series. Manuscript.
- Bluhm, M. and Krahnen, J. P. (2014). Systemic risk in an interconnected banking system with endogenous asset markets, *Journal of Financial Stability* **13**: 75–94.
- Brechmann, E., Hendrich, K. and Czado, C. (2013). Conditional copula simulation for systemic risk stress testing, *Insurance: Mathematics and Economics* **53**: 722–732.
- Chan-Lau, J., Chuang, C., Duan, J. and Sun, W. (2016). Banking network and systemic risk via forward-looking partial default correlation. Manuscript.
- Das, S. R. (2016). Matrix metrics: Network-based systemic risk scoring, *Journal of Alternative Investments: Special Issue on Systemic Risk* **18**(4): 41 – 55.
- Diebold, F. X. and Yilmaz, K. (2014). On the network topology of variance decompositions: Measuring the connectedness of financial firms, *Journal of Econometrics* **182**(1): 119–134.
- Dungey, M. and Gajurel, D. (2015). Contagion and banking crisis: International evidence for 2007-2009, *Journal of Banking and Finance* **60**: 271–283.
- Fan, Y., Härdle, W. K., Wang, W. and Zhu, L. (2016). Single index based CoVaR with very high dimensional covariates, *Journal of Business Economics and Statistics* . DOI:10.1080/07350015.2016.1180990.
- Franke, J., Härdle, K. and Hafner, C. (2015). *Statistics of Financial Markets: An Introduction*, 4 edn, Springer Verlag, Heidelberg, eBook ISBN 978-3-642-54539-9, Softcover ISBN 978-3-642-54538-2, DOI: 10.1007/978-3-642-54539-9.

- Han, H., Linton, O., Okac, T. and Whang, Y.-J. (2016). The cross-quantilogram: Measuring quantile dependence and testing directional predictability between time series, *Journal of Econometrics* **193**(1): 251–270.
- Härdle, W. K., Wang, W. and Yu, L. (2016). TENET: Tail-Event driven NETwork risk, *Journal of Econometrics* **192**(2): 499–513.
- Hautsch, N., Schaumburg, J. and Schienle, M. (2014). Financial network systemic risk contributions, *Review of Finance* **19**(2): 685–738.
- Koenker, R. (2005). *Quantile Regression*, Cambridge University Press.
- Koenker, R. and Bassett, G. (1978). Regression quantiles, *Econometrica* **46**(1): 33–50.
- Koenker, R. and Machado, J. (1999). Goodness of fit and related inference porocesses for quantile regression, *Journal of American Statistical Association* **94**(448): 1296–1310.
- Koenker, R. and Xiao, Z. (2006). Quantile autoregression, *Journal of the American Statistical Association* **101**(475): 980 – 990.
- Laeven, L., Ratnovski, L. and Tong, H. (2015). Bank size, capital, and systemic risk: Some international evidence, *Journal of Banking and Finance* **192**(2): 499 – 513.
- McCauley, R. and Zukunft, J. (2008). Asian banks and the international interbank market, *BIS Quarterly Review* **June**: 67 – 79.
- Ng, S. (2006). Testing cross-section correlation in panel data using spacings, *Journal of Business and Economic Statistics* **24**(1): 12–23.
- Tran, N. M., Burdejová, P., Osipenko, M. and Härdle, W. K. (2016). Principal component analysis in an asymmetric norm, *SFB 649 Discussion Paper 2016-040*, submitted to JRSS. <http://sfb649.wiwi.hu-berlin.de/papers/pdf/SFB649DP2016-040.pdf>.
- Xu, X., Chen, C. Y.-H. and Härdle, W. K. (2016). Dynamic credit default swaps curve in a network topology, *submitted to Journal of Financial Econometrics* . SFB DP 2016-059.
- Zhu, X., Pan, R., Li, G., Liu, Y. and Wang, H. (2017). Network vector autoregression, *Annals of Statistics* . In print.

Zhu, X., Wang, W., Wang, H. and Härdle, W. (2016). Network quantile autoregression, *submitted to Journal of American Statistical Association* . SFB DP 2016-050.

# SFB 649 Discussion Paper Series 2017

For a complete list of Discussion Papers published by the SFB 649, please visit <http://sfb649.wiwi.hu-berlin.de>.

- 001 "Fake Alpha" by Marcel Müller, Tobias Rosenberger and Marliese Uhrig-Homburg, January 2017.
- 002 "Estimating location values of agricultural land" by Georg Helbing, Zhiwei Shen, Martin Odening and Matthias Ritter, January 2017.
- 003 "FRM: a Financial Risk Meter based on penalizing tail events occurrence" by Lining Yu, Wolfgang Karl Härdle, Lukas Borke and Thijs Benschop, January 2017.
- 004 "Tail event driven networks of SIFIs" by Cathy Yi-Hsuan Chen, Wolfgang Karl Härdle, Yarema Okhrin, January 2017.

**SFB 649, Spandauer Straße 1, D-10178 Berlin**  
**<http://sfb649.wiwi.hu-berlin.de>**

This research was supported by the Deutsche  
Forschungsgemeinschaft through the SFB 649 "Economic Risk".

